The International Journal of Advanced Manufacturing Technology (2019) 101:2761–2770
https://doi.org/10.1007/s00170-018-2966-x

ORIGINAL ARTICLE

Effect of environmental temperature on dynamic behavior of an adjustable preload double-nut ball screw

De-Shin Liu[1] · Pen-Chen Lin[1] · Jheng-Jie Lin[1] · Chuen-Ren Wang[1] · Ting-Nung Shiau[1]

Received: 27 July 2018 / Accepted: 30 October 2018 / Published online: 11 December 2018

Abstract

The dynamic behavior of adjustable preload double-nut ball screw has been investigated by finite element simulation model under different environmental temperature conditions. The simulations focus specifically on the effects of the ambient temperature (5~55 °C) on the torque acting on the flange of the ball screw mechanism at rotational speeds of 50~1000 rpm. The environment temperature effect was less studies to discuss the heat deformation issue of ball screw. The validity of the simulation results is confirmed by comparing the predicted torque values with the experimental measurements. It is shown that the torque decreases logarithmically with an increasing temperature due to a change in the expansion coefficients of the ball screw mechanism components and a reduction in the viscosity of the ball screw lubricant. In particular, for a rotational speed of 1000 rpm, the torque reduces by approximately 75.6% as the environmental temperature is increased from 5 to 55 °C. However, for a constant temperature, the torque decreases with an increasing rotational speed due to centrifugal effects. For a low-rotational speed of 100 rpm, a good qualitative agreement is observed between the simulated torque and the measured torque at higher temperatures. However, in the low-temperature regime (e.g., 5 °C), the simulated torque is around 47.6% lower than the measured value.

Keywords Environmental temperature · Adjustable preload double-nut ball screw

1 Introduction

Double-nut ball screw mechanisms are widely used in the machine tool industry. However, in practical applications, backlash frequently occurs as a result of structural deflection, positioning errors, or clearances between the nut and screw groove surfaces. As a result, the accuracy and reliability of the ball screw mechanism are reduced. To improve the positioning performance, an appropriate preload force must therefore be applied to minimize the backlash and increase the contact stiffness. However, the positioning accuracy may still be degraded by environmental temperature effects, which cause a change in the material properties of the various ball screw mechanism components and the viscosity of the ball screw lubricant. The dynamic behavior of ball screw mechanisms has attracted significant attention in the literature. Olaru et al. [1] conducted a numerical investigation into the frictional moment between the screw and the nut during rotation. Sobolewski [2] presented a model for predicting the impact force produced by the balls of the ball screw drive mechanism during the transient stage of motion as a function of the screw and ball diameters and the rotational speed, respectively. Mu and Feng [3] examined the effects of gyroscopic and centrifugal forces on the dynamic behavior of high-speed ball screws and showed that the contact force acting on the ball surface decreased with an increasing spin speed. Chen et al. [4] examined the shape error of ball screws with compliance effects and showed that the error increased with an increasing ball screw acceleration due to a greater moment of inertia. Weule and Frank [5] improved the positioning performance of a ball screw mechanism through an additional preload control process. Verl and Frey [6, 7] showed that the preload force increases linearly with an increasing spin speed. Wei et al. [8] developed a mathematical model for describing the effects of preload and lubrication on the dynamic behavior of a single-nut double-cycle ball screw. Reynolds [9] constructed a

✉ De-Shin Liu
imedsl@ccu.edu.tw

[1] Advanced Institute of Manufacturing with High-tech Innovations and Department of Mechanical Engineering, National Chung Cheng University, 621 Chia Yi, Taiwan, Republic of China

Coulomb friction model to predict the dynamic ball rotation behavior in a ball screw system with lubrication effects. Harris [10] analyzed the frictional and sliding behaviors of the ball bearings in a ball screw mechanism as a function of the bearing force and moment. Hamrock [11] investigated the effects of the lubricant viscosity on the dynamic behavior of the ball bearings in a ball screw system. Verl and Frey [12] used a strain gauge measurement approach to calculate the average moment acting on the flange of a ball screw. Wang et al. [13] performed a numerical and experimental investigation into the effects of the ball screw parameters on the dynamic response of a ball screw mechanism. Xia et al. [14] showed that the dynamic behavior and positioning performance of ball screws are extremely sensitive to the ambient temperature. Xu et al. [15] investigated the effects of the temperature distribution, thermal deformation, and air cooling performance on the dynamic behavior of a ball screw mechanism and showed that the positioning accuracy was significantly improved given the use of an air cooling system. Brouwer [16] examined the effects of changes in the lubricant viscosity on the dynamic response of a ball screw system.

The published literature contains many analytical models for predicting the reaction force and frictional force in ball screw systems. However, the validity of most of these models has not been demonstrated experimentally. Accordingly, in a previous study [13], the present group confirmed the validity of the proposed analytical model by comparing the simulation results for the reaction force and torque acting on the flange of the nut under run-in conditions (100 rpm) with the equivalent experimental results. The simulations in [13] considered a constant ambient temperature of 25 °C. Accordingly, in the present study, the numerical model developed in [13] is used to investigate the dynamic response of an adjustable double-nut ball screw mechanism under ambient temperatures varying from 5~55 °C, and rotational speeds of 50~1000 rpm are different in more references. The validity of the numerical results is confirmed via a comparison with the experimental measurements. This study provides the close and stable environmental temperature field to study the thermal effect and different to many references.

2 Experimental apparatus

Figure 1 presents a photograph of the thermal box used to regulate the ambient temperature in the experimental measurement process. The five points indicated in Fig. 1 denote the temperature measurement position. Those points can reflect the environment temperature value of thermal box. If the wrong position has been chosen, the field of environmental temperature can be inaccurate. For each considered temperature in the range of 5~55 °C, the experimental system was allowed to warm for 30 min in order to obtain steady-state conditions before the torque measurements were obtained.

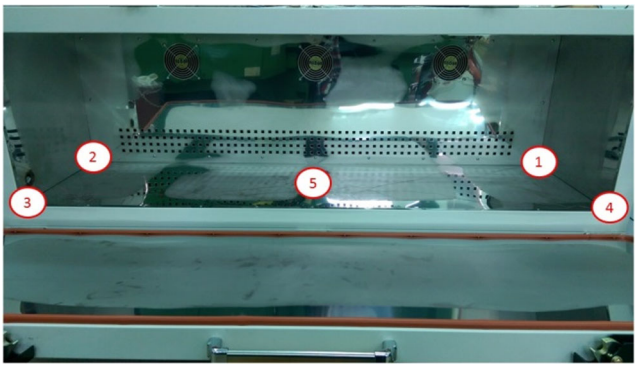

Fig. 1 Photograph of thermal test box

As shown in Fig. 2, the main components of the ball screw apparatus included a commercial double-nut ball screw, a linear guideway, a coupling, a torque sensor, a thermocouple, and a Panasonic A5 servo-motor from the integration cell by HIWIN. The maximum travel distance of the nut was around 1000 mm. The torque sensor was positioned in such a way as to measure the torque of ball screw with or without preload. In performing the experiments, the torque acting on the flange of the nut was measured using a hand-held digital force gauge and torque sensor. Table 1 shows the detailed specification of the ball screw from [17]. Figure 3 shows the hydraulic preload system used in the present experiments to set the required preload on the ball screw mechanism. Figure 4 is the explosion drawing of the preload table. The components include the nut, base, pad, load cell, platform, nut, and cylinder. The required components of the preload table are listed in Fig. 5; the hydraulic preload system created the preload by compressor, than use the control valve to adjust the pressure.

3 Formulation and model

The three topics of dynamic model include the model, experiment, and lubrication effect, respectively. The detail descriptions are presented as follows.

3.1 Ball screw model

In general, it is computationally expensive to treat each of the components of the double-nut ball screw mechanism as an elastic body. Thus, in constructing the analytical model of the ball screw mechanism in [13], only the surface grooves

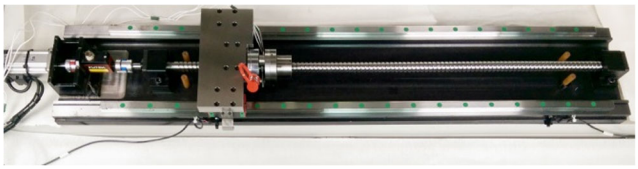

Fig. 2 Ball screw system.

Table 1 Parameters of the double-nut ball screw

Parameters of HIWIN© ball screw	
Steel ball diameter (mm)	3.175
Pitch circle diameter (mm)	25.6
Lead of screw (mm)	10
Lead angle of screw (deg)	7.09

of the screw and nuts were considered to undergo elastic deformation. By contrast, the steel balls were treated as rigid bodies since they have a far greater hardness than the surface grooves. Similarly, the return tubes of the nuts were also treated as rigid bodies since the end-cap deformation is significantly lower than that of the surface grooves. Such assumptions are reasonable for the ambient temperature conditions considered in [13], i.e., 25 °C. However, for the simulations performed in the present study, with temperatures ranging from 5~55°C, the rigid-body assumption can no longer be applied. Hence, all of the components of the ball screw mechanism (e.g., the ball screw and nuts) were considered to be elastic bodies. For simplicity, however, the nonlinear time-varying characteristics of the lubrication effect were ignored.

The simulations considered an end-cap recirculation double-nut ball screw mechanism with two sets of steel balls. The material parameters of the ball screw are listed in Table 2. Note that for reasons of simplicity, the differences among the material properties of the screw, nuts, and balls, respectively, were assumed to be sufficiently small to be ignored [13].

Figures 6 show the finite element (FE) models of the screw and nut in the double-nut ball screw mechanism, respectively. In general, the mesh type of a FE model plays a key role in determining the simulation results. In the present study, the steel balls, nut flanges, and surface grooves of the nuts and screw were meshed using tetrahedron and wedge elements, while the remainder of the model was meshed using hexahedron brick elements. Furthermore, as shown in Fig. 7, the model was meshed using a non-uniform grid size. In particular, a more refined grid was applied in the groove regions of the model in order to better capture the effects of the greater stress and deformation in these particular regions of the ball screw mechanism. The dynamic behavior of the double-nut ball screw mechanism was evaluated by means of ABAQUS

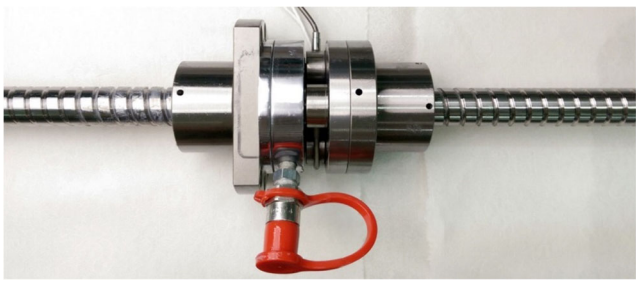

Fig. 3 Variable preload ball screw

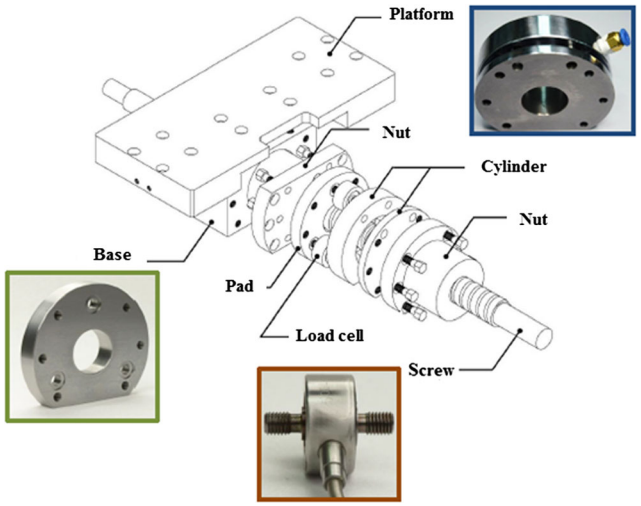

Fig. 4 The exploded drawing of preload ball screw system

6.13© simulations performed with a general contact setting for the surface elements. The screw was assigned a single rotational degree of freedom, while the nuts were assigned both translational and rotational degrees of freedom. In addition, the steel balls were assumed to move freely since, in practical applications, their motion between the nut inner surface and the screw outer surface is unconstrained. As shown in Fig. 8, the flanges of the nuts were assumed to be stationary, thereby resisting rotation of the nuts and producing a corresponding torque. Finally, the desired value of the ambient temperature for each simulation was input directly to the ABAQUS simulation model as a thermal boundary condition.

3.2 Experimental validation

As described in [13], the validity of the FE model was evaluated by comparing the simulation results for the torque acting on the flange of the double-nut ball screw mechanism at the run-in speed of 100 rpm with the measured value obtained using a manual torque sensor. The corresponding results are shown in Figs. 9 and 10, where the solid trace indicates the torque profile

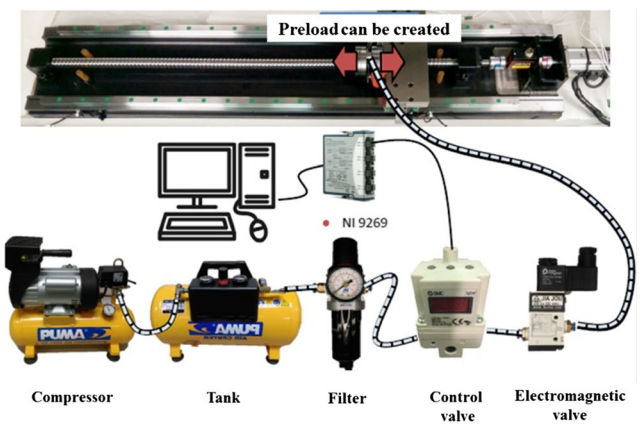

Fig. 5 The preload system of ball screw

Table 2 Material parameters of double-nut ball screw

Parameters	Value
Young's modulus (GPa)	207
Poisson ratio	0.3
Density (g/cm^3)	7.8

and the red dotted lines show the upper and lower bounds of the experimental torque measurements. It is seen that other than the initial moments following startup (i.e., t < 0.015 sec), the simulated torque values all fall within the measured range. Thus, the basic validity of the analytical model is confirmed. The force control and displacement control are different from the constraint. The force control limits the force value at the constant force; similarly, the displacement control limits the displacement value. The results are same with together.

3.3 Frictional moment and lubrication effect

From the Olaru's study [1], the tangential force and moment from the lubrication effect were studied by more references. This study cited the hydrodynamic rolling force due to Poiseuille flow of the lubricant contact as showed in Fig. 11. The formulation is presented as follows.

$$F_R = 2.86 \cdot E \cdot R \cdot x^2 \cdot k^{0.348} \cdot G^{0.022} \cdot U^{0.66} \cdot W^{0.47} \tag{3.1}$$

The parameter of U is dependence with the lubrication effect and presented as follows.

$$U = \frac{\eta_0 \cdot v}{E \cdot R_x} \tag{3.2}$$

Where η_0 is the viscosity of lubricant at the atmospheric pressure. The pressure force due to the horizontal component of the lubricant pressure in the direction is illustrated as follows.

$$F_{Pb} = 2F_R \frac{R_R}{R_R + R_b} \tag{3.3}$$

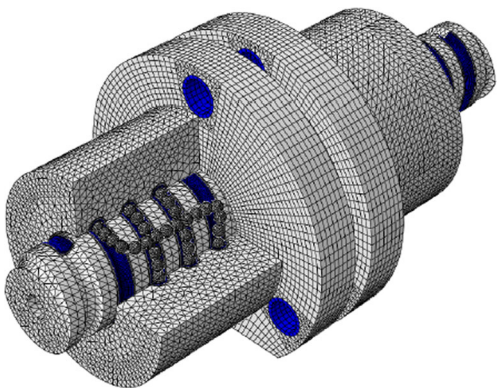

Fig. 6 The mesh model of ball screw (blue region: flexible body)

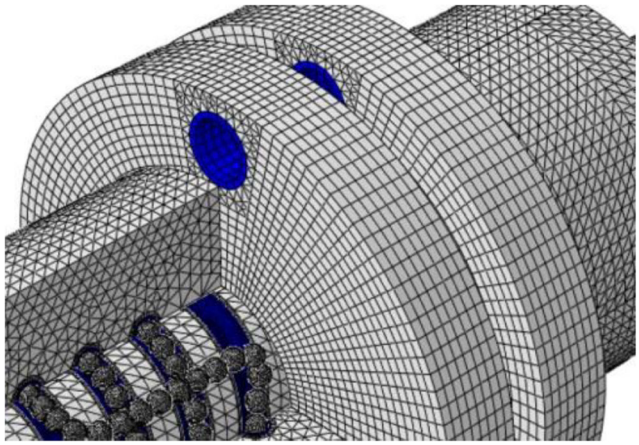

Fig. 7 Non-uniform grid size on flange of double-nut ball screw (Include tetrahedron and wedge elements)

The curvature friction moment is employed as a constant coefficient of friction, and a Hertzian distribution of the contact pressure can be presented as showed in Figs. 12 and 13. The formulation can be presented as follows.

$$M_C = 0.1 \cdot \mu_m \cdot \frac{Qa^2}{Rd} \cdot \left(1 - 5 \cdot Y^3 + 3 \cdot Y^5\right) \tag{3.4}$$

Where, Rd is the deformed radius in ball-race contact, Y is the dimensionless distance between the point of pure rolling and the center of contact ellipse, and a is the semi-major axis of contact ellipse.

The lubrication effect is considered in the ball screw with the above as the equivalent force and moment among Eqs. (3.1) to (3.4). Therefore, the dynamic response of ball screw system has already included the lubrication effect. The detail illustration can be referred in reference [1]. Table 3 is presented the parameters of ball screw with lubrication effect to use in the simulation.

4 Effects of ambient temperature on flange torque and preload torque

Having validated the numerical model under run-in conditions, a series of simulations were performed to investigate

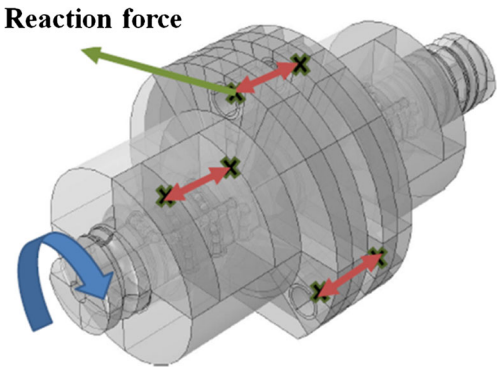

Fig. 8 Boundary condition and setting of ball screw

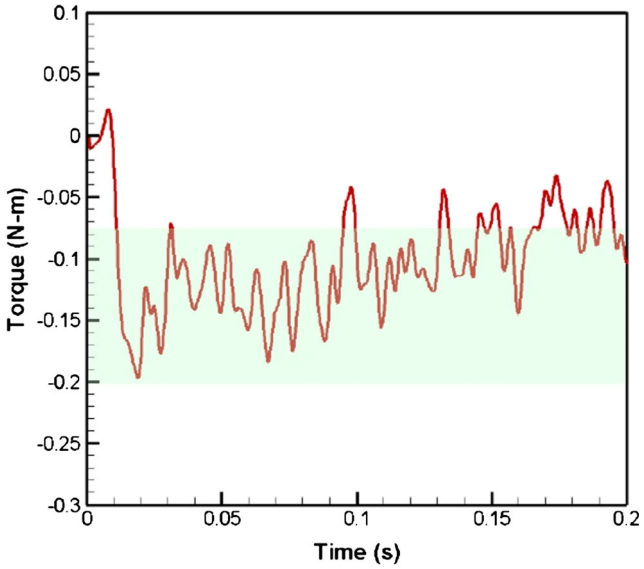

Fig. 9 Simulation results for time history of torque with force control acting on the flange of nut during run-in period

the effects of the environmental temperature (5~55 °C) and rotational speed (50~1000 rpm) on the torque acting on the nut flange. Further simulations were then performed to investigate the effect of the temperature on the preload torque.

4.1 Effects of ambient temperature on reaction torque acting on the flange

Figures 14 and 15 present the simulation results obtained for the variation of the torque acting on the flange with the ambient temperature as a function of the rotational speed in the forward and reverse directions, respectively. For convenience, the average torque values under the simulated temperature and

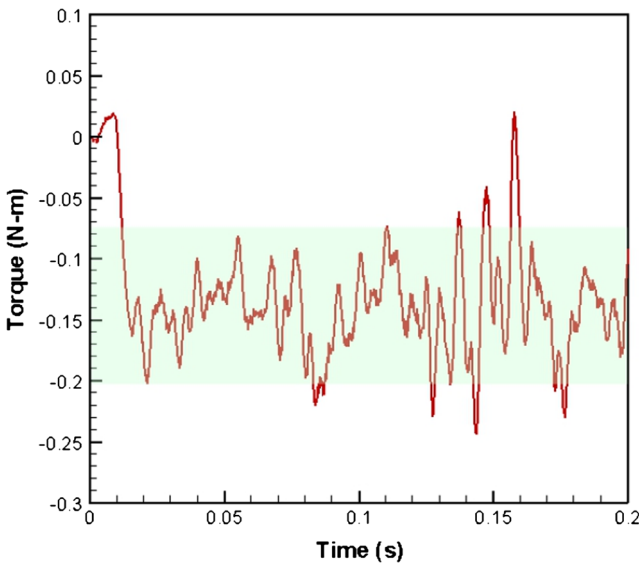

Fig. 10 Simulation results for time history of torque with displacement control acting on the flange of nut during run-in period

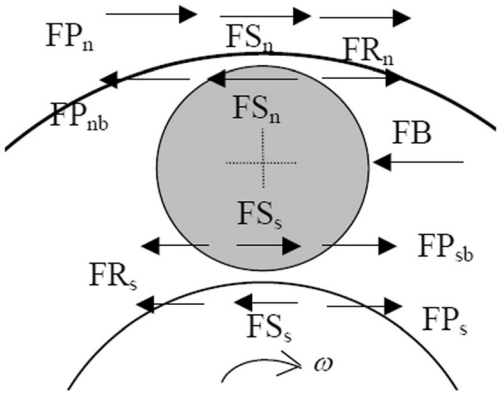

Fig. 11 The force acting on the ball and on the races in a ball screw system

speed conditions are summarized in Tables 4 and 5. As shown in Fig. 14, the torque reduces with an increasing ambient temperature for all values of the rotational speed. Taking a temperature of 30 °C for reference purposes, it is seen that the torque increases by around 10~20% for each reduction of 5 °C in the temperature. By contrast, for each 5 °C increase in the temperature beyond 30 °C, the torque reduces by approximately 2~10%. In other words, the torque and temperature are related via a logarithmic relationship.

Taking the maximum rotational speed of 1000 rpm for illustration purposes, the torque is found to reduce by approximately 75.6% as the ambient temperature is increased from 5~55 °C. In part, the reduction in torque with an increasing temperature can be attributed to a change in the material properties of the ball screw mechanism components as the temperature increases.

Figure 15 shows that the torque also decreases with an increasing temperature when the ball screw mechanism is operated in the reverse direction. In general, the results presented in Figs. 14 and 15 show that for a given temperature, the torque increases with an increasing rotation speed. Actually, it is because of the greater centrifugal force generated by the

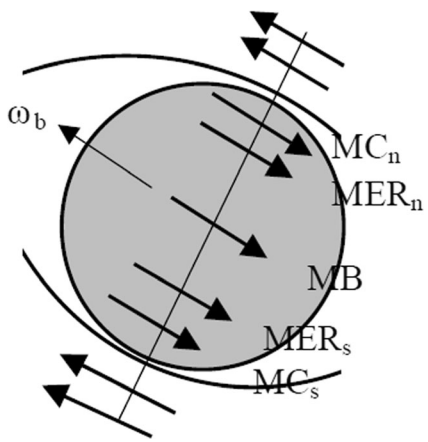

Fig. 12 The moments acting on the ball and on the two races in a ball screw system

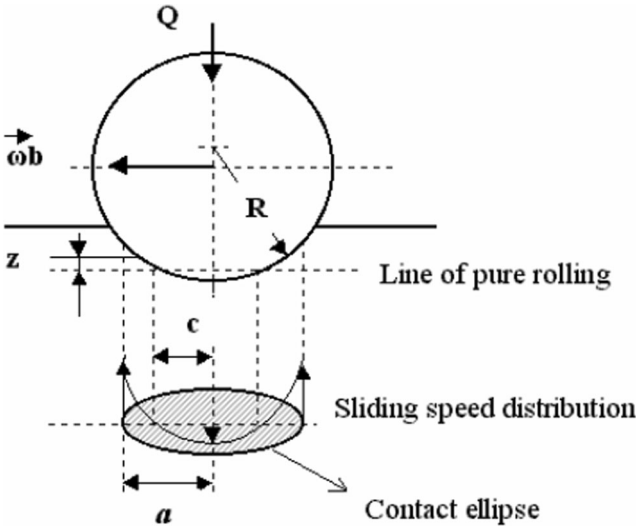

Fig. 13 Sliding speed distribution in a ball race contact ellipse

ball bearings at a higher speed. Compared with Figs. 14 and 15, when ball screw rotates to the CCW direction, the steel ball must resist the gravity, the gravity force will increase the friction force as shown in Fig. 16. It means that the torque not only friction force but also the extra friction force by gravity. In other words, the gravity force will decrease the friction force in the CW direction case as shown in Fig. 17. However, Brouwer [16] showed that the viscosity of typical ball screw lubricants decreases by around 33% for each 9 °C increase in the temperature (see Fig. 18). Thus, the reduction in the torque acting on the flange at a higher temperature can also be attributed to a reduced viscosity of the lubricant.

Figures 19 and 20 compare the simulated values of the torque obtained at different temperatures with the experimental measurements given rotational speeds of 100 rpm (low-

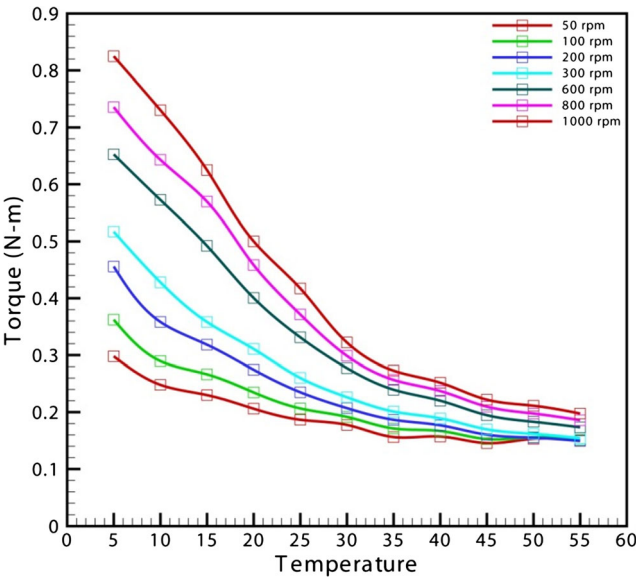

Fig. 14 Simulated torque acting on flange as function of ambient temperature and rotational speed in forward direction

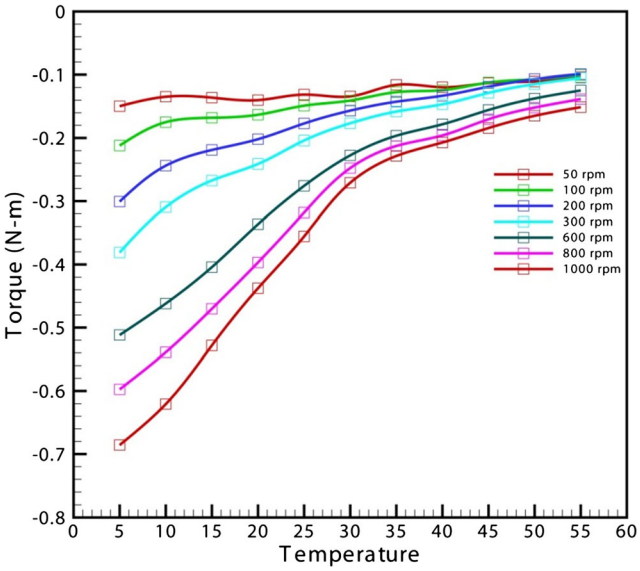

Fig. 15 Simulated torque acting on flange as function of ambient temperature and rotational speed in reverse direction

rotational speed regime) and 1000 rpm (high-rotational speed regime), respectively. For the low-rotational speed regime, the simulated value of the torque at an ambient temperature of 5 °C is around 47.6% lower than the experimental measurement. This result arises since the simulations ignore the expansion effect of the ancillary components of the ball screw system, e.g., the bearing, the coupling, and the motor. However, the simulated torque values approach the experimental measurements as the temperature increases. For the high-rotational speed regime (Fig. 20), the simulated torque values are consistently lower than the experimental values for all values of the temperature. However, the two sets of results demonstrate a similar decreasing tendency with an increasing ambient temperature. This finding is reasonable since, for a high-rotational speed, the expansion effects of the ancillary components on the simulated torque are outweighed by the inertia effects produced by the rotating steel balls. In other words, at the rotating speed of 1000 rpm case, the simulation case has the same tendency with the experiment of the ball screw table; it means under high-rotational speeds, the torque acting on the flange is dominated by the frictional moment induced by the bearing rather than the preload moment.

4.2 Frictional moment induced by preload

A further series of simulations were performed to examine the effect of the ambient temperature on the preload torque given a rotational speed of 100 rpm. As shown in Fig. 19, the simulation results were compared with those obtained in two different experimental conditions, namely, a variable preload ball screw case (i.e., the ball screw mechanism was not installed on the table) and a variable preload ball screw system case (i.e., the ball screw mechanism was installed on the table). In order

Table 3 Average torque as function of ambient temperature and forward rotation speed (unit: N-m)

PCD dimension(mm)	25.6
Steel ball dimension(mm)	3.175
Lead(mm)	10
Viscosity coefficient(Pa.s)	0.2
Press-viscosity coefficient(Pa)	10^{-8}

Table 4 Average torque as function of ambient temperature and reverse rotation speed (unit: N-m)

rpm °C	1000	800	600	300	200	100
5	0.824827	0.735671	0.652603	0.51696	0.455845	0.362188
10	0.730394	0.643069	0.572684	0.428035	0.358292	0.28966
15	0.624946	0.569581	0.49204	0.358192	0.318331	0.266351
20	0.500021	0.458428	0.400486	0.310795	0.274392	0.234707
25	0.41723	0.371371	0.331239	0.260065	0.234968	0.206577
30	0.322248	0.298801	0.277284	0.226287	0.207113	0.191738
35	0.272805	0.256712	0.239474	0.201088	0.186621	0.171307
40	0.251843	0.237258	0.220229	0.189168	0.176945	0.166944
45	0.222006	0.209773	0.194721	0.169714	0.160319	0.152603
50	0.211365	0.1976	0.183052	0.161809	0.155097	0.15583
55	0.197634	0.185919	0.173377	0.154213	0.149283	0.151377

Table 5 Average torque as function of ambient temperature and reverse rotation speed. (unit:N-m)

rpm °C	1000	800	600	300	200	100
5	-0.68567	-0.5975	-0.51171	-0.38095	-0.30071	-0.21198
10	-0.62078	-0.53894	-0.4619	-0.30948	-0.24387	-0.17487
15	-0.52819	-0.4702	-0.40421	-0.26733	-0.21897	-0.16798
20	-0.43765	-0.39677	-0.33634	-0.24116	-0.20189	-0.16314
25	-0.35559	-0.31808	-0.27587	-0.20396	-0.17701	-0.1488
30	-0.27098	-0.2477	-0.22758	-0.17669	-0.15663	-0.14066
35	-0.22851	-0.21265	-0.19645	-0.15813	-0.14248	-0.12729
40	-0.20718	-0.19593	-0.17828	-0.14657	-0.13305	-0.1242
45	-0.18423	-0.17027	-0.15557	-0.12854	-0.11869	-0.11216
50	-0.16482	-0.15177	-0.13739	-0.11465	-0.10686	-0.1069
55	-0.15118	-0.13842	-0.12468	-0.10507	-0.0989	-0.10055

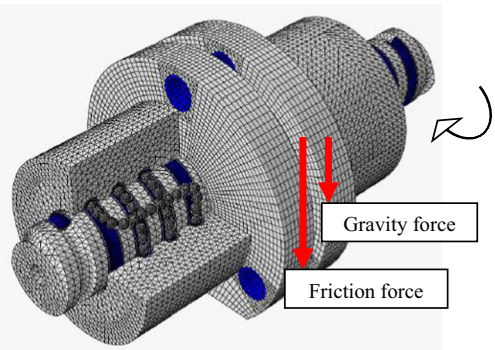

Fig. 16 The summation of gravity and friction force in CCW direction (forward motion) of ball screw rotation

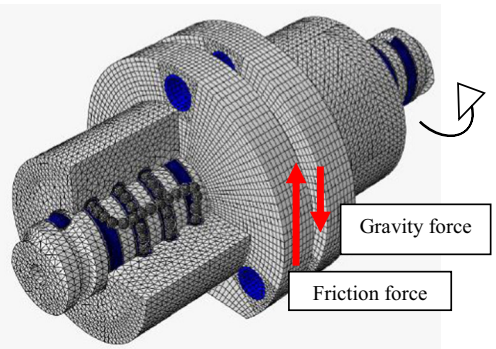

Fig. 17 The summation of gravity and friction force in CW direction (backward motion) of ball screw rotation

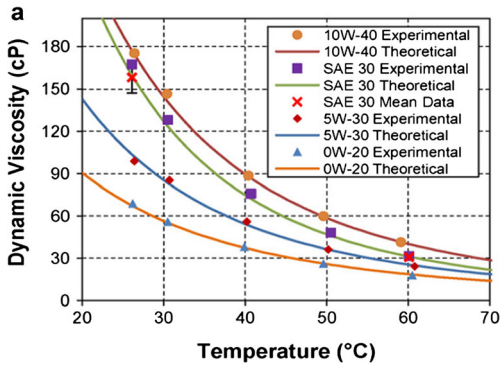

Fig. 18 Variation of lubricant viscosity with temperature (reproduced from [16])

to distinguish among the three different sets of results in the following discussions, the FEM simulations are denoted as case A, the variable preload ball screw case (non-installed with the ancillary components) is denoted as case B, and the variable preload ball screw system case (installed with the ancillary components) is denoted as case C. As shown in Fig. 21, the static preload tendencies of case A and case B are very similar over the entire temperature range. For case C, the measured preload values are similar to those of case A and case B for ambient temperatures less than 30 °C. However, for temperatures greater than 30 °C, the measured preload increases greatly and deviates notably from case A and case B results. This finding is reasonable since, while cases A and B consider a free-standing ball screw mechanism, case C considers the ball screw mechanism to be installed on the table. Hence, the preload is determined not only by the ball screw mechanism but also by the ancillary components of the table (in particular, the linear guideway and the bearing). Generally speaking, these components have a higher hardness and Young's modulus than the components of the ball screw mechanism and thus experience a greater velocity of

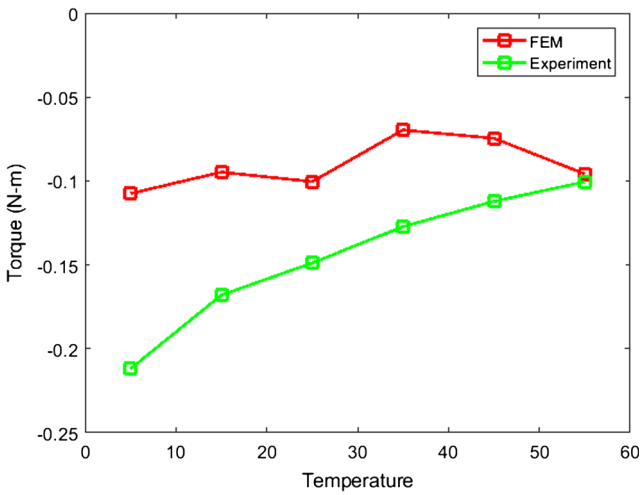

Fig. 19 Simulated and experimental values for torque acting on flange as function of ambient temperature given low-rotational speed of 100 rpm

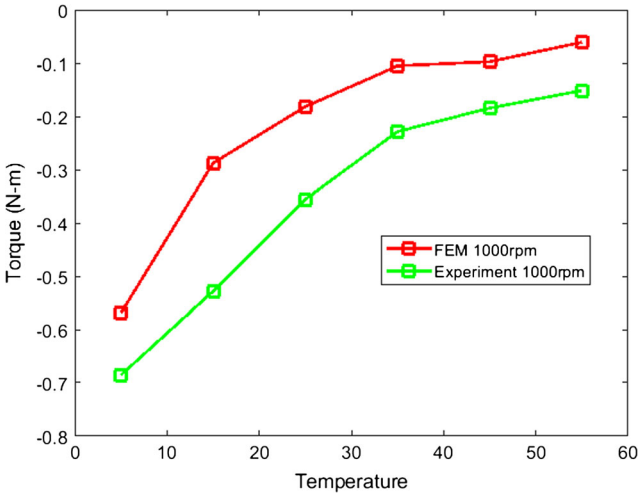

Fig. 20 Simulated and experimental values of torque acting on flange as function of ambient temperature given high-rotational speed of 1000 rpm

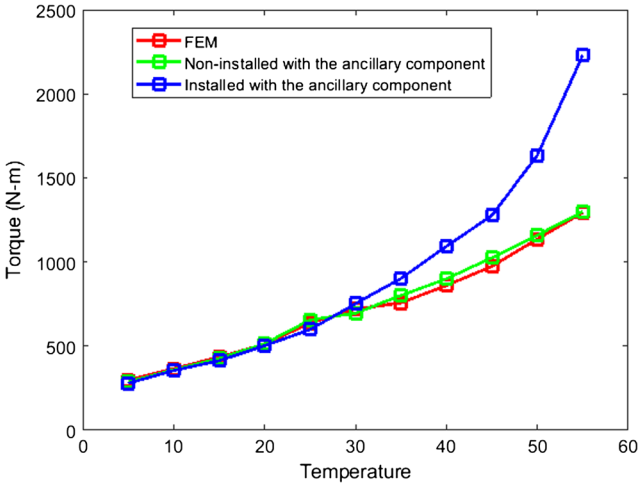

Fig. 21 Variation of preload torque as function of screw rotation speed in ambient temperature given rotational speed of 100 rpm

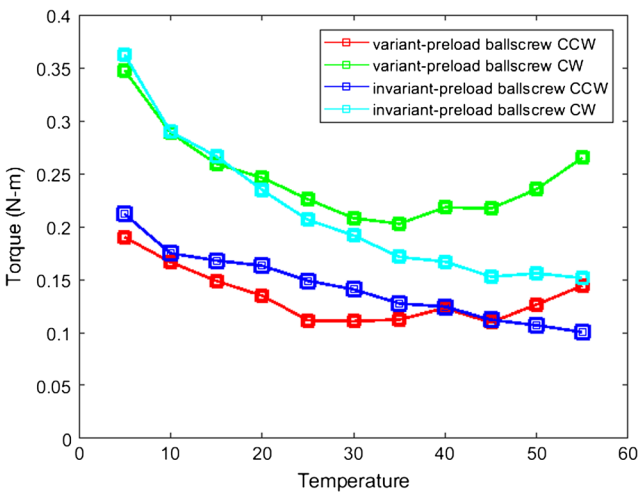

Fig. 22 Variation of invariant-preload torque and variable preload torque with temperature given forward and reverse directions of rotation

expansion under elevated temperatures. Consequently, the preload increases notably with an increasing temperature compared to the case where these ancillary components are not taken into account.

Figure 22 shows the torque measurements obtained in case B and case C given forward and backward rotations of the ball screw, respectively. The results confirm that the preload torque increases in case C at temperatures higher than 30 °C due to the expansion effect of the ancillary components of the table. The discrepancy of high rotating speed and low rotating speed between the two sets of results arises since the simulations ignore the expansion effect of the ancillary components of the ball screw system, including the bearing, the coupling, and the motor. Given a high-rotational speed of 1000 rpm, the simulation results for the variation of the torque with the temperature are in reasonable qualitative agreement with the experimental measurements for all values of the ambient temperature since the torque is dominated by the inertial effect of the steel balls (i.e., the expansion effects of the ancillary components have a relatively lower impact on the magnitude of the torque acting on the flange). Finally, for temperatures higher than 30 °C, the measured preload torque acting on the flange of an installed ball screw mechanism is higher than that acting on the flange of a free-standing ball screw mechanism due to the expansion effects of the ancillary components of the table (e.g., the linear guideway and bearing).

5 Conclusion

This study has performed a numerical and experimental investigation into the torque exerted on the flange of an adjustable preload double-nut ball screw mechanism under ambient temperatures of 5~55 °C and rotational speeds of 50~1000 rpm. The main results can be summarized as follows:

(1) During forward rotation, the torque acting on the flange decreases logarithmically with an increasing temperature. For a rotational speed of 1000 rpm, the torque reduces by approximately 75.6% as the temperature increases from 5~55 °C.
(2) For a low-rotational speed of 100 rpm, the simulated torque is around 47.6% lower than the experimental torque under low-temperature conditions (5 °C). The discrepancy between the two results arises since the simulations ignore the expansion effect of the ancillary components of the ball screw system (e.g., the bearing, the coupling, and the motor).
(3) For a high-rotational speed of 1000 rpm, the simulation results for the torque acting on the flange are in good qualitative agreement with the experimental results for all values of the ambient temperature. In other words, at high-rotational speeds, the torque acting on the flange is dominated by the frictional moment induced by the bearing rather than the preload moment.
(4) For temperatures lower than 30 °C, the simulated value of the preload moment acting on the flange of a non-installed ball screw mechanism is in good agreement with the measured value obtained for a ball screw mechanism installed on a working table. However, at temperatures higher than 30 °C, the torque acting on the flange of the installed ball screw mechanism is higher than that acting on the free-standing ball screw mechanism due to the expansion effects of the ancillary components of the table (in particular, the guideway and bearing). The adjustable preload can be based on the different condition to change the preload; this behavior can save the motor energy to create the green manufacturing industry.

Acknowledgements The authors thank the AIM-HI of National Chung Cheng University and HIWIN© Technologies Corporation of Taiwan for their help in this study.

References

1. Olaru D, Puiu GC, Balan LC, Puiu V (2004) A new model to estimate friction torque in a ball screw system. Prod Eng 333–346
2. Sobolewski JZ (2012) Vibration of the ball screw drive. J Eng Fail Anal 24:1–8
3. Mu SG, Feng XY (2011) Study of the dynamic characteristic of high-speed screw. J Hunan Univ 38:25–29
4. Chen JS, Huang YK, Cheng CC (2004) Mechanical model and contouring analysis of high-speed ball-screw drive systems with compliance effect. J Adv Manuf Technol 24:241–250
5. Weule H, Frank T (1999) Advantage and characteristics of a dynamic feeds axis with ball screw drive and driven nut. J Ann CIRP 48:303–306
6. Verl A, Frey S (2010) Correlation between feed velocity and preloading in ball screw drives. J CIRP Ann Manuf Technol 59: 429–433
7. Verl A, Frey S, Heinze T (2014) Double-nut ball screw with improved operating characteristics. J CIRP Ann Manuf Technol 63: 361–364
8. Wei CC, Lin JF, Horng JH (2009) Analysis of a ball screw with a preload and lubrication. J Tribol Int 42:1816–1831
9. Reynolds O (1876) On rolling-friction. Philos Trans R Soc Lond 166:155–174
10. Harris T (1971) Ball motion in thrust-loaded, angular-contact ball bearings with coulomb friction. ASME Trans J Lubr Technol 93: 32–38
11. Hamrock BJ (1994) Fundamentals of fluid film lubrication. McGraw-Hill, New York

12. Verl A, Frey S (2010) Correlation between feed velocity and preloading in ball screw drives. CIRP Ann Manuf Technol 59: 429–432
13. Wang CR, Liu DS, Huang CH, Shiau TN (2016) Numerical investigation into dynamic behavior of adjustable preload double-nut ball screw. J Mech Sci Technol 30:4489–4496
14. Xia JY, Hu YM, Wu B, Shi TL (2009) Research on thermal dynamics characteristics and modelling approach of ball screw. Int J Adv Manuf Technol 43:421–430
15. Xu ZZ, Liu XJ, Kim HK, Shin JH, Lyu SK (2011) Thermal error forecast and performance evaluation for an air-cooling ball screw system. Int J Mach Tool Manu 51:605–611
16. Brouwera MD, Guptab LA, Sadeghia F, Peroulisb D, Adamsa D (2012) High temperature dynamic viscosity sensor for engine oil. Sensors Actuators A Phys 173:102–107
17. Technical Manual of Ball Screw of HIWIN (2018) 599TE21-1898 22-31.